

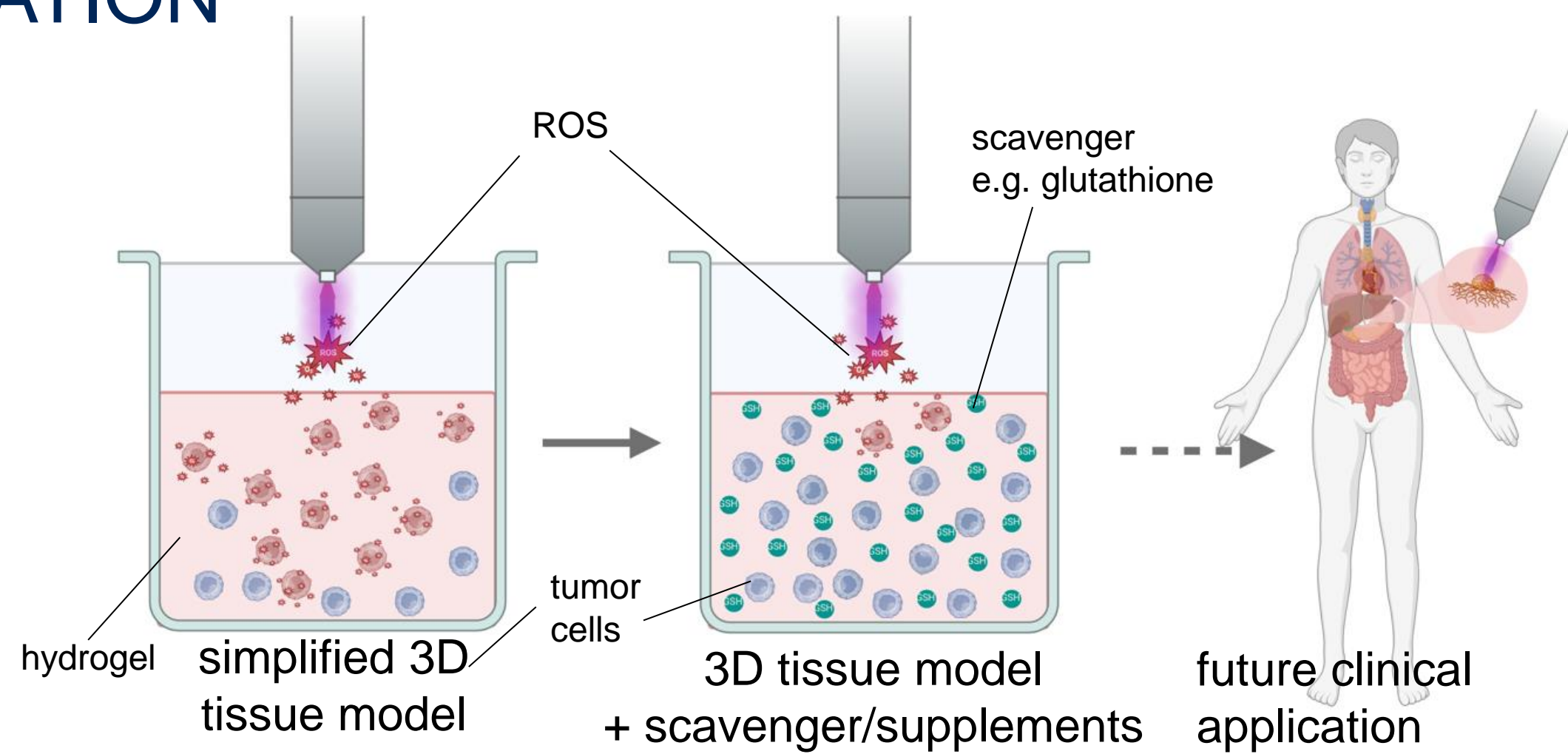
Tino Pritzkow<sup>1,2</sup>, Alice Martinet<sup>1,3</sup>, Lea Miebach<sup>1</sup>, Stephan Kersting<sup>2</sup>, Sander Bekeschus<sup>1,3</sup>

<sup>1</sup> ZIK *plasmatis*, Leibniz Institute for Plasma Science and Technology (INP), Greifswald, Germany

<sup>2</sup> Department of General, Visceral, Thoracic, and Vascular Surgery, Greifswald University Medical Center, Germany

<sup>3</sup> Department of Dermatology and Venerology, Rostock University Medical Center, Germany

## MOTIVATION



Medical gas plasma therapy has been successfully applied to many types of cancers in preclinical models and also palliative treatment regimes in head and neck cancer patients [1-2]. This innovative treatment approach generates a versatile mix of reactive oxygen (ROS) and nitrogen species (RNS) that have been linked to a variety of anti-tumor effects. However, these effects are potentially influenced by large number of different molecules in vivo, which have not been addressed by previous studies. To gain better insight into the processes that underlies anti-tumor effects of gas plasma-derived ROS/RNS, we here aim to characterize substances and tissue-like properties that significantly influence these effects in a new easily accessible hydrogel-based tissue model.

## 1. DEVELOPMENT OF A NEW 3D TISSUE MODEL

### Gel composition screening

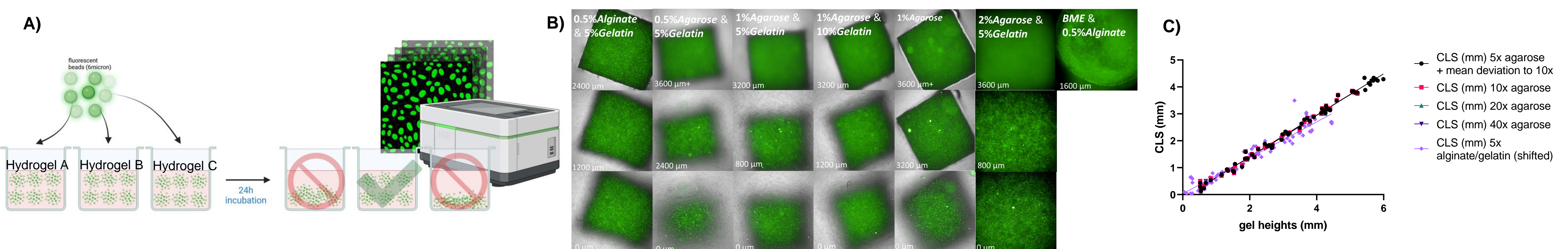


**Fig. 1.** **A)** Scheme of gel screening: 6 micrometer-sized fluorescent polystyrene beads were embedded within different hydrogel types, incubated for 24h at 24°C/5% CO<sub>2</sub> before high-content imaging was performed to determine optimal imaging conditions. **B)** High-content imaging of hydrogels with embedded fluorescent beads after 24h incubation to examine spatial distribution of beads, (with paper cuttings on top for improved surface focus). **C)** Z-axis calibration curve to verify penetration depth imaging data with actual height differences (CLS data vs. caliper-measured heights).

### Cell line screening

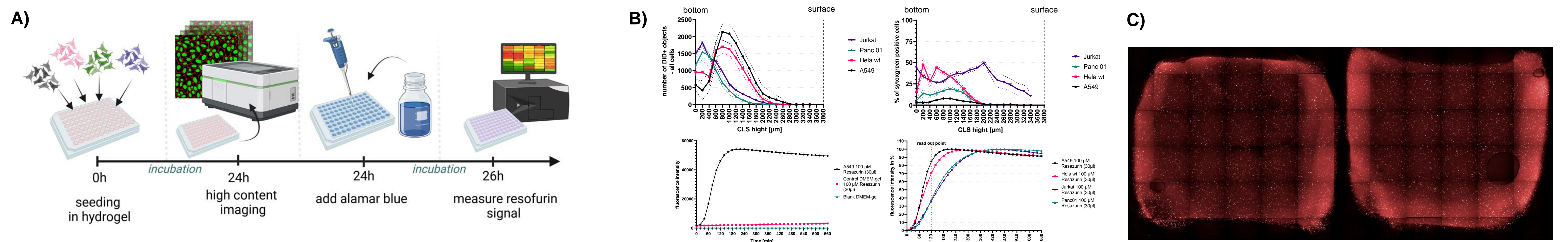


**Fig. 2.** **A)** Scheme: various cancer cell lines were stained with DiD (cell tracer) and Sytox Green (cell death dye) and seeded into hydrogel. High-content imaging was performed after 24h of incubation as well as resazurin-conversion assays to determine metabolic activity of tumor cells within the gel. **B)** Top: High-content imaging was performed on 0.5%Alginate/5%Gelatin-hydrogel and the distribution of all DiD-positive cells (all cells) over z-axis within the gel plotted (left), percentage of Sytox Green-positive (dead) cells within the DiD positive cells distributed over z-axis (right); bottom: time-lapse for resorufin signals (Tecan M200 microplate reader) to assess metabolic activity of tumor cells dynamically; raw data + controls for A549 (left), normalized to highest value per gel-control (right). **C)** High content image: cutting surface of hydrogel with DiD-stained Jurkat cells after 24h incubation.

### Gas plasma treatment

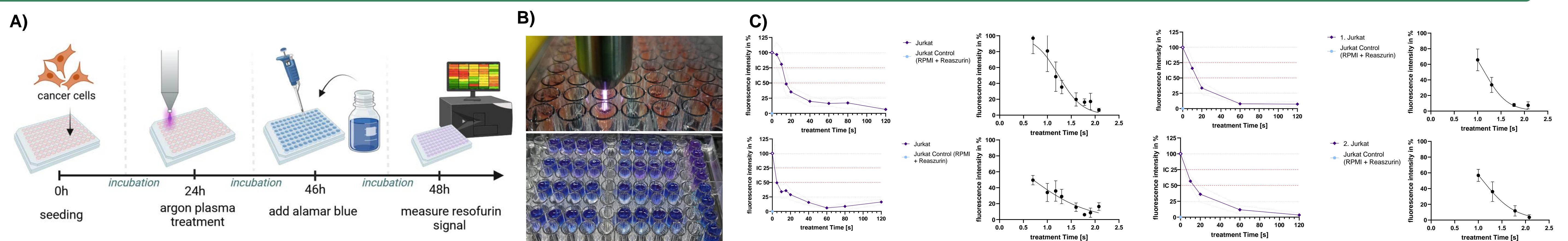
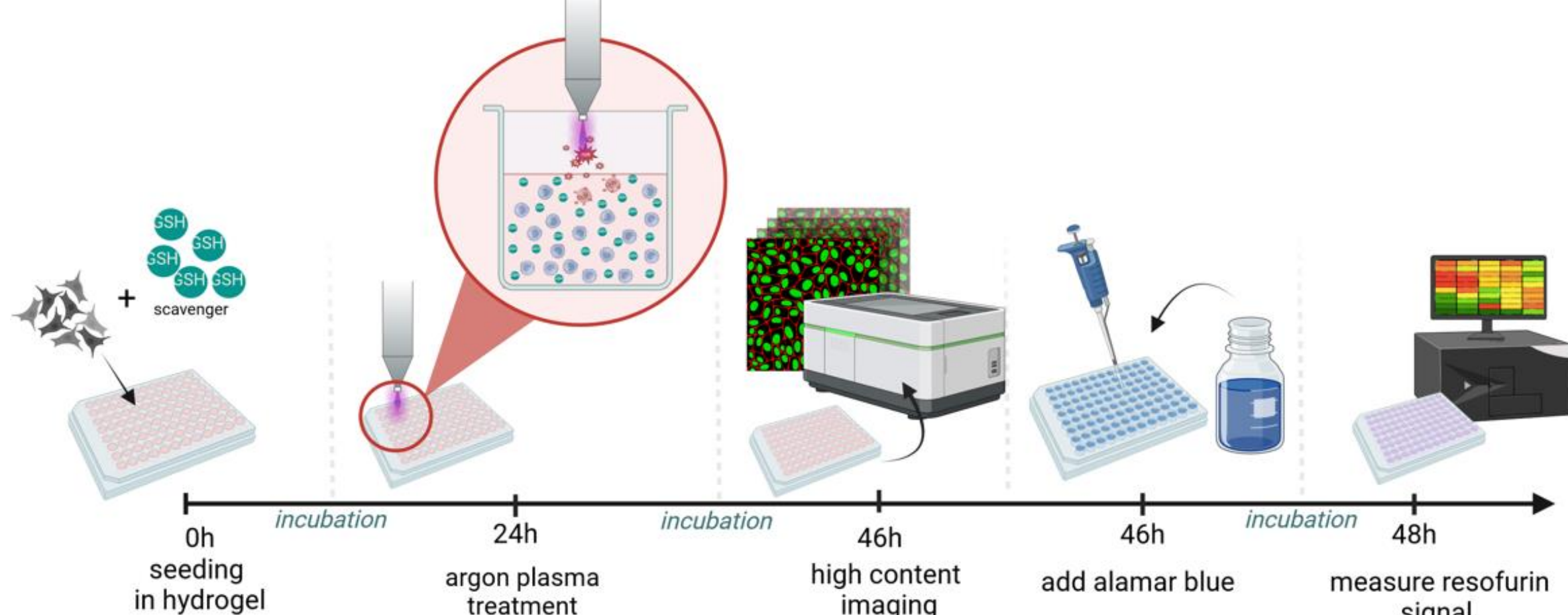


**Fig. 3.** **A)** Scheme of gas plasma treatment: embedding cancer cells in hydrogels and treating them with an argon plasma jet after 24h of incubation. After another incubation period (22h), the metabolic activity of tumor cells was analyzed. **B)** Top: image of argon plasma treatment, bottom: hydrogel with Jurkat cells and 100µM resazurin on top after 2h incubation. **C)** Biological replicates of metabolic activity assay after argon plasma treatment: on gel-control and highest value-normalized data (left) and transformed data, log x-axis and nonlinear regression for IC25 determination (right).

## 2. IMPACT OF ROS-SCAVENGERS AND OTHER SUPPLEMENTS



In the next steps of the project, we will characterize the penetration of reactive species in hydrogel-based tissue models in the presence of various ROS scavengers and additional supplements. Furthermore, the influence of altered ROS penetration dependent on hydrogel composition on cellular oxidation and toxicity to hydrogel-embedded tumor cells. Later, similar effects should be studied in more complex and commercially available hydrogel-based tissue models.

**Fig. 4.** Scheme of future experimental steps for ongoing project.

### References:

- [1] Bekeschus, S. et al. (2020). *Advanced Science*  
[2] Metelmann, H.-R., et al. (2018). *Clinical Plasma Medicine*